RAPID COMMUNICATIONS

PHYSICAL REVIEW E VOLUME 59, NUMBER 4 APRIL 1999

High efficiency coupling and guiding of intense femtosecond laser pulses in preformed plasma channels in an elongated gas jet

S. P. Nikitin, I. Alexeev, J. Fan, and H. M. Milchberg
Institute for Physical Science and Technology, University of Maryland, College Park, Maryland 20742

(Received 31 August 1998)

We report coupling and guiding of pulses of peak power up to 0.3 TW in 1.5-cm-long preformed plasma waveguides, generated in a high repetition rate argon gas jet. Coupling of up to 52% was measured for 50-mJ, ~110-fs pulses injected at times longer than 20 ns, giving guided intensities up to $\sim 5\times 10^{16}$ W/cm^2. For short delays between waveguide generation and pulse injection, pulse shortening occurred, with this effect reduced either by increasing delay or injecting a prepulse into the waveguide. There is excessive taper at the waveguide ends, which results from reduced heating at the ends of the jet by the waveguide generation pulse. [S1063-651X(99)51704-2]

PACS number(s): 52.40.Nk, 52.35.Mw, 52.40.Db

The optical guiding of intense laser pulses in plasmas has several important applications, including laser-driven electron acceleration and x-ray generation [1]. Guiding has been demonstrated both in the nonlinear self-guiding regime [2] and in preformed plasma channels, which have been produced either in high voltage capillary discharges [3] or by thermally driven laser-induced plasma expansion [4]. In the latter approach, channels were produced in the focus of an axicon in an ambient background gas, with neutral gas extending in front of the channel entrance and beyond the exit. Maximum coupling efficiency was ~70%, limited to moderate intensity ($<10^{15}$ W/cm^2) optical guiding [4]. Later experiments at higher laser intensity (5×10^{15} W/cm^2) showed that optical field ionization of neutral gas in advance of the channel entrance caused severe refraction of the injected pulse before it entered the channel, resulting in reduced coupling efficiency of less than 30% and refraction-induced pulse shortening [5]. The refraction problem is a serious limitation for applications such as laser wakefield generation, which requires guided intensities in excess of $\sim 10^{18}$ W/cm^2 [1].

The absence of gas from the region in advance of the waveguide entrance would be expected to reduce the refraction problem and make higher injected intensities possible, and to this end we designed a high repetition rate gas jet in which to produce the plasma waveguide [6]. The jet nozzle is fed by a pulsed solenoid valve and in the experiments reported here, the nozzle orifice was an elongated slot 1.5 cm long and 0.75 mm wide. The nozzle end face was tapered to minimize its obstruction of the axicon beam used to generate the plasma waveguide. The obstruction has a minimal effect on the gas breakdown [6], and this observation is supported by calculations that show that the obstruction reduces the peak intensity by the fraction of the obstructed beam energy (<10%) with little disruption to the Bessel field profile in the focus [7].

The plasma waveguides in the experiments reported here were produced in the 1.7-cm-long line focus of a 25° base angle axicon using 200–300 mJ, 100 ps, $\lambda = 1.064$ μm pulses (peak intensity $\sim 4\times 10^{13}$ W/cm^2) from a neodymium-doped yttrium aluminum garnet (Nd:YAG) regenerative amplifier/power amplifier system [8]. Argon gas was used in the jet, with a valve backing pressure of 33 atm and a gas puff full width at half maximum (FWHM) of 550 μs, with the laser pulse arriving at the temporal peak of the puff. The axicon

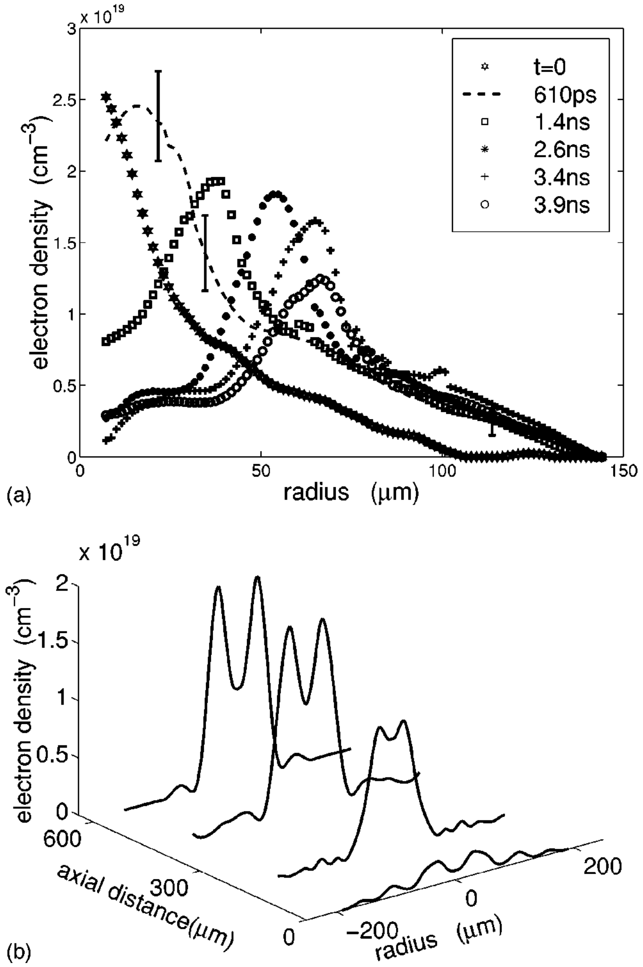

FIG. 1. (a) Time resolved electron density profiles of the evolving plasma waveguide, where $t=0$ refers to the center of the 225 mJ waveguide generation pulse. (b) End region of plasma waveguide, showing tapering of the electron density profile. Probe delay $=3.0$ ns.

1063-651X/99/59(4)/3839(4)/$15.00 PRE 59

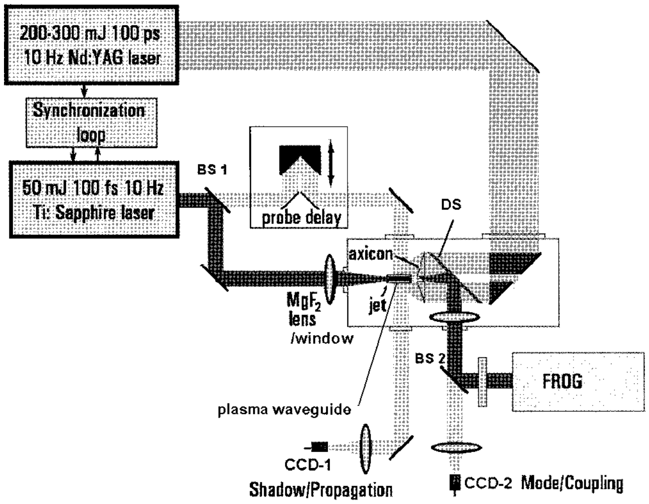

FIG. 2. Experimental setup for femtosecond pulse guiding experiments.

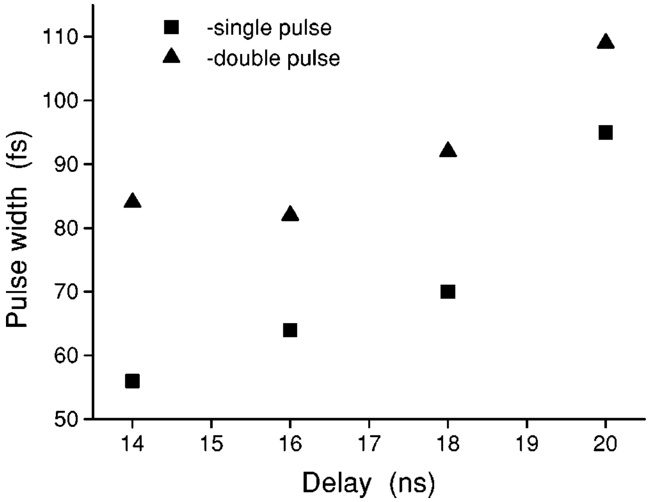

FIG. 3. FROG measurement of waveguide output pulse width vs delay for the injection of (i) single 50-mJ, 110-fs pulse and (ii) prepulse/main pulse combination (8-mJ, 110-fs prepulse; 42-mJ, 110-fs main pulse; separation=4 ns), where delay is the time between channel generation and main pulse injection.

line focus was aligned 2 mm from the nozzle orifice and overfilled the length of the gas region. Folded wavefront interferometry was used to measure the spatial profiles of neutral gas density (shown in Ref. [6]) and plasma waveguide electron density from the jet, using variably delayed $\lambda=532$-nm probe pulses obtained from frequency doubling $\lambda=1064$-nm pulses from the Nd:YAG system. A sequence of electron density profiles near the midsection of the waveguide is shown in Fig. 1(a), obtained from Abel inversion of the phase plots extracted from the interferograms [6]. The time scales for channel evolution are similar to those of our earlier backfill experiments, and the channels are as axially uniform as in the backfill case [6,9].

The degree of taper of the end of the plasma waveguide is important for coupling considerations. Figure 1(b) shows electron density profiles as a function of axial distance at the end of the waveguide at 3 ns after waveguide generation. The electron density profile falloff to the end of the guide takes place over ~300 μm, longer than the ~150-μm falloff in the case of gas backfill [9]. At this delay, the central electron density at ~300 μm from the end is about two times higher than near the waveguide midsection. This most likely results from reduced inverse bremsstrahlung laser heating as the gas density falls off at the end of the jet. Since the laser-plasma heating rate scales as N^2, the temperature scales as N and the collisional ionization rate scales as $N^2 \exp(-\chi/kT)$, where N is the density and χ is the ionization potential, we would expect reduced heating and ionization, along with reduced channel expansion in the jet edge region. An end density falloff distance of ~0.5 mm was estimated from both shadowgraphy and by focusing a high intensity Ti:sapphire laser pulse (100 fs, 20 mJ) into the end of the jet and imaging the resulting visible recombination radiation, which is proportional to the gas density at such short pulse width.

Guiding experiments were performed with a high power femtosecond Ti:sapphire laser system (10 Hz, 50 mJ, 780 nm, 100 fs), synchronized to the Nd:YAG waveguide generating laser as described in Ref. [5]. The experimental setup is shown in Fig. 2. The femtosecond pulses were focused with a MgF$_2$ lens at *f*/15 through a MgF$_2$ window in the experimental chamber. The vacuum focus intensity FWHM was 30 μm, approximately twice diffraction limited. A small portion of the main pulse (~5%) was split off with a pellicle (BS1) and directed to a delay line for femtosecond time-resolved shadowgrams which were captured with camera CCD-1. After the jet (waveguide) interaction region, the guided femtosecond pulse was reflected to the chamber exit by a dichroic beam splitter (DS), after which it was split by another pellicle (BS2) and directed to a frequency-resolved optical gating (FROG) [10] diagnostic, and to a microscope objective and camera CCD-2 for images the channel exit plane. The beam splitter DS also transmits the 1064-nm waveguide generation pulse from the opposite direction.

Figure 3 shows waveguide output pulsewidth measurements made with the FROG diagnostic for injection with either single 110-fs, 50-mJ pulses or a prepulse/main pulse combination (first to second pulse energy ratio of 1:5, pulse widths of 110 fs, and a pulse separation of 4 ns) of total energy 50 mJ.The double pulse was produced by injecting the Ti:sapphire regenerative amplifier with two variably separated seed pulses from the oscillator The waveguides were produced in argon under the conditions of Fig. 1. For the double pulse injection, the FROG measurement effectively registers the second pulse alone, since the raw signal level is proportional to the cube of intensity [10]. It is seen that the measured pulse shortening is reduced for longer de-

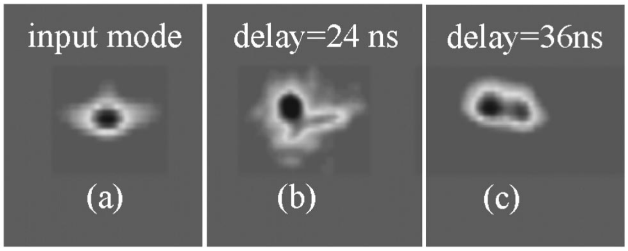

FIG. 4. (a) Mode image for vacuum case (FWHM=30 μm); guided mode for (b) 24-ns delay (FWHM=35 μm) and (c) 36-ns delay.

lays (for both single and double pulses) between waveguide generation and injection, and at all delays the shortening is less for the double pulse case. The smaller amount of shortening for double pulse injection reinforces our earlier conclusion [5,11] that the origin of the shortening is refraction at the channel entrance, and indicates that the 20% level prepulse preionizes residual gas and low charge-state ions at the channel entrance, reducing the refracting effect of ionization on the main pulse. The reduction in shortening as injection delay increases for both single and double pulses is consistent with increased channel width at the entrance, resulting in better capture of refracted light and decreased interaction with the less ionized gas at the channel radial periphery. We note that the waveguides of this experiment are not long enough (at the measured electron density) for the negative group velocity dispersion of plasma to be responsible for the maximum 30–40 % shortening observed.

The FROG traces show only a very small level of blue shifting for the guided pulses, even in the presence of shortening. A very slight increase in blue shift with delay (not plotted) suggests that at early delay, light refracted through ionization at the channel entrance is diverted outside the channel acceptance and, at later delay, more of this light is captured by the channel. The contribution of ionization in the main part of the channel to blue shifting of the guided pulse is negligible. An estimate of the average degree of ionization Z, induced by the 100-ps waveguide generation pulse, is found by dividing the central electron density at early times in the channel evolution by the known gas density [9]. For the waveguide conditions shown in Fig. 1(a), $Z \approx 8$, which indicates that Ne-like argon is the dominant species in the waveguide. The approximate intensity threshold for optical field ionization from Ne-like to F-like argon is $\sim 10^{18}$ W/cm^2 [12], so that further ionization by the guided pulse would not be expected at our peak guided intensity of less than $\sim 10^{17}$ W/cm^2 (see below).

The vacuum focal spot and guided mode images are shown in Fig. 4. In contrast to the case of waveguides produced in a gas backfill, where the injected pulse delay for efficient coupling at this f number is no more than 5–6 ns [4], typical minimum delays of 10–15 ns are required for efficient coupling to the jet channel. This results from the longer taper at the end of the gas jet waveguides, which requires longer expansion times for efficient pulse injection. Coupling efficiency for both single and double pulse injection at delays longer than 20 ns is slightly better than 50%, measured by integrating the exit image and dividing by the integral of the vacuum spot image. The coupling efficiency remains at $\sim$50% out to $\sim$40 ns, where it begins to slowly decrease. At 24-ns delay, typical single mode output is shown (FWHM 35 μm), and it is larger than the vacuum spot, owing to the channel expansion. At an even longer delay of 36 ns, $m=1$ mode structure appears with the onset of two lobes. Depending on the delay, pulse shortening down to $\sim$70 fs occurs (as shown in Fig. 3), resulting in peak powers transmitted up to $\sim$0.3 TW, and guided intensity up to $\sim 5 \times 10^{16}$ W/cm^2. However, at these rather large spot diameters, there is only 8–9 Rayleigh lengths of guiding.

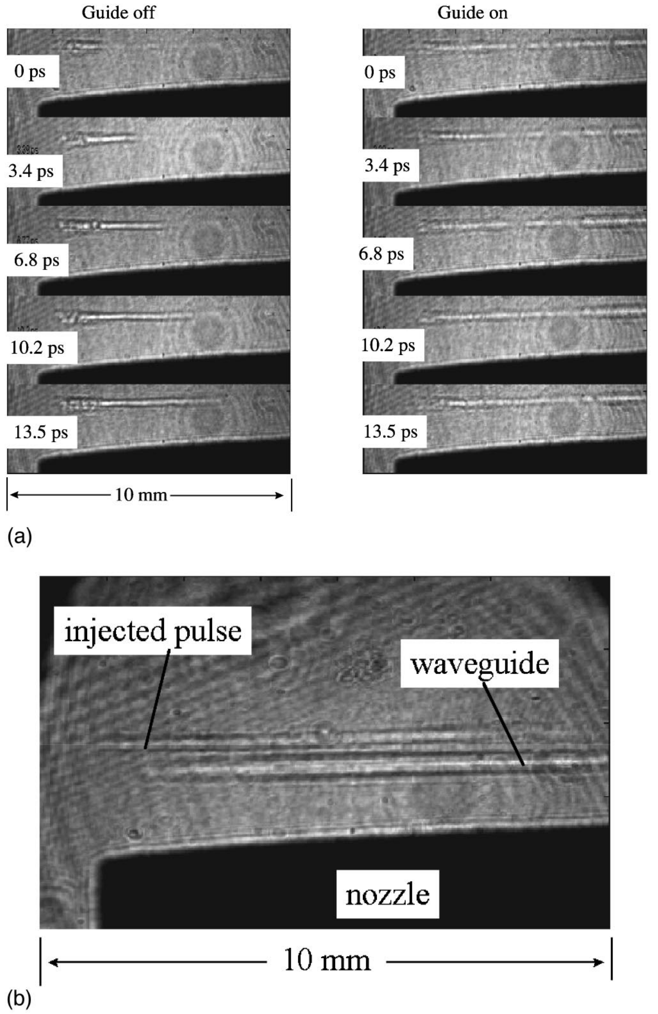

FIG. 5. Time sequential shadowgrams showing coupling of femtosecond pulses to the elongated gas jet alone (guide off) and to the plasma waveguide generated in the gas jet (guide on). The waveguide conditions are those of Fig. 1, and the injection delay is 24 ns. The dark region is the shadow of the nozzle. The delays on the figure refer to the probe delay after the pulse enters the jet. (b) Shadowgram showing misaligned coupling between the injected pulse and the waveguide. Probe delay after femtosecond pulse enters jet is 17 ps.

Femtosecond time-resolved shadowgrams were used to examine the coupling and propagation of injected pulses near the waveguide entrance. Figure 5(a) shows a sequence of shadowgrams for the injected pulse propagating into the gas jet (with the waveguide off). The abrupt onset of ionization (within $\sim$0.5 mm) is seen at the jet entrance, with the ionization front propagating from left to right at the speed of light. The relatively collimated looking ionization region results from the on-axis intensity of the pulse remaining sufficiently high for ionization of neutral Ar. With the waveguide on, there is little apparent effect on the shadowgram induced by the guided pulse, as is consistent with the FROG measurements, which indicated negligible additional ionization in the waveguide. Figure 5(b) is a shadowgram of vertically misaligned coupling between the injected pulse and the waveguide, showing that $\sim$0.5 mm of gas at the entrance to the jet is insufficiently ionized by the 100-ps waveguide generation pulse. This is the source of the residual refraction-induced shortening seen in the FROG measurements of the waveguide output.

In conclusion, we have demonstrated optical guiding of up to 0.3-TW pulses in plasma waveguides generated in a high repetition rate pulsed gas jet, achieving high coupling efficiencies of $\sim$50%. The existence of a finite scale length in gas density of $\sim$0.5 mm at the end of the jet results in reduced efficiency of inverse bremsstrahlung heating and ionization at the jet edge by the 100-ps waveguide generation pulse. This results in both an excessive waveguide taper and a reduced level of ionization at the end of the waveguide. There are two consequences of this. First, longer delays are needed before injection to achieve efficient coupling. Second, pulse shortening from ionization induced refraction at the waveguide entrance is observed. The shortening is reduced with double pulse injection or single pulse injection at longer delay. For efficient injection and guiding of the fundamental mode at a small spot size over a larger number of Rayleigh lengths, future work will require increasing the heating and ionization at the jet edge.

The authors thank T. Antonsen for useful discussions. This work was supported by the U.S. Department of Energy (Grant No. DEF G0297 ER 41039).

---

[1] C. J. Joshi and P. B. Corkum, Phys. Today **48**, 36 (1995); T. Tajima and J. Dawson, Phys. Rev. Lett. **43**, 267 (1979).

[2] A. B. Borisov *et al.*, Phys. Rev. Lett. **68**, 2309 (1992); P. Monot *et al.*, *ibid.* **74**, 2953 (1995); K Krushelnick *et al.*, *ibid.* **78**, 4047 (1997); R. Wagner *et al.*, *ibid.* **78**, 3125 (1997); J Fuchs *et al.*, *ibid.* **80**, 1658 (1998).

[3] Y. Erlich, C. Cohen, A. Zigler, J. Krall, P. Sprangle, and E. Esarey, Phys. Rev. Lett. **77**, 4186 (1996).

[4] C. G. Durfee, J. Lynch, and H. M. Milchberg, Phys. Rev. E **51**, 2368 (1995); C. G. Durfee and H. M. Milchberg, Opt. Lett. **19**, 1937 (1994); Phys. Rev. Lett. **71**, 2409 (1993).

[5] S. P. Nikitin, T. M. Antonsen, T. R. Clark, Yuelin Li, and H. M. Milchberg, Opt. Lett. **22**, 1787 (1997).

[6] J. Fan, T. R. Clark, and H. M. Milchberg, Appl. Phys. Lett. **73**, 3064 (1998).

[7] Z. Bien and T. M. Antonsen (unpublished).

[8] T. R. Clark, Ph.D. thesis, University of Maryland, 1998 (unpublished).

[9] T. R. Clark and H. M. Milchberg, Phys. Rev. Lett. **78**, 2373 (1997).

[10] D. J. Kane and R. Trebino, Opt. Lett. **18**, 823 (1993).

[11] S. P. Nikitin, Y. Li, T. M. Antonsen, and H. M. Milchberg, Opt. Commun. **157**, 139 (1998).

[12] S. Augst, D. Strickland, D. Meyerhofer, S. L. Chin, and J. H. Eberly, Phys. Rev. Lett. **63**, 2212 (1989).